บรรณานุกรม

1. Q. Wan, Q. H. Li, Y. J. Chen, T. H. Wang, X. L. He, J. P. Li and C. L. Lin. *Applied Physics Letters*. 2004, 3654: 84.

2. X. Jiaqiang, C. Yuping, and S. Jianian. *Journal of Nanoscience and Nanotechnology*. 2006, 248-253(6): 6.

3. ภานุพัฒน์ ชัยวร"การเตรียมวิสเกอร์ซิงก์ออกไซด์ด้วยวิธีการปลูกจากไอเพื่อใช้เป็นเซนเซอร์ เอทานอล" วิทยานิพนธ์วิทยาศาสตรมหาบัณฑิต สาขาวิชาฟิสิกส์ประยุกต์ มหาวิทยาลัยเชียงใหม่ (2550)

4. H. Iwanaga, M. Fujii, and S. Takeuchi. *J. Cryst. Growth.*. 1993, 275-280: 134.

5. J.Q. Hu and Y. Bando. *Appl. Phys. Lett.*. 2003, 1401-1403: 82.

6. J. Cheng, R. Guo, and Q.M. Wang. *Appl. Phys. Lett.*. 2004, 5140-5142: 85.

7. A.Tsukazaki, A. Ohtomo, T. Onuma, M. Ohtani, T. Makino, M. Sumiya, K. Ohtani, S.F. Chichibu, S. Fuke, Y. Segawa, H. Ohno, H. Koinuma, and M. Kawasaki. *Nat. Mater.*. 2005, 42-48: 4.

8. Z.W. Pan, Z.R. Dai, and Z.L. Wang. *Science*. 2001, 1947-1949: 291.

9. Y. Li, G.W. Meng, L.D. Zhang, and F. PhillippAppl. *Phys. Lett.*. 2000, 2011–2013: 76.

10. X.H. Sun, S. Lam, T.K. Sham, F. Heigl, and A. Ju1rgensen. *J. Phys. Chem. B.*. 2005, 3120-3125: 109.

11. J.J. Wu, S.C. Liu, C.T. Wu, K.H. Chen, and L.C. Chen. *Appl. Phys. Lett.*. 2002, 1312-13124: 81.

12. M.H. Huang, Y.Y. Wu, H. Feick, N. Tran, E. Webber, and P.D. Yang. *Adv. Mater.*. 2001, 113-116: 13.

13. University at Buffalo. "Method Safely Deposits Novel Metal Oxide Thin Films on Substrates". [Online]. Available: *www.physorg.com/news108830724.html (2007, September 12)*

14. Z. Xu, J.Y. Hwang, B. Li, X. Huang, and H. Wang. "The Characterization of Various ZnO Nanostructures Using Field-Emission SEM". [Online]. Available: *www.tms.org/pubs/journals/jom/0804/xu-0804.html (No date)*

15. "Chemists measure copper levels in zinc oxide nanowires" [Online]. Available: *nanotechnologytoday.blogspot.com/2008_03_01_a... (2008, March 8)*

16. University of Ulster "The Nanotechnology and Integrated Bio Engineering Centre-Image Gallery"[Online]. Available : *www.nibec.ulster.ac.uk/about_us/gallery.php (2007)*

17. Michigan Technological University "ZnO Nanotubes" [Online]. Available: *www.phy.mtu.edu/yap/gallery.html (No date)*

18. Feri Adriyanto "Nanorods" [Online]. Available: *feriadriyanto.staff.uns.ac.id/.../ (2008)*

19. "Nanonails" [Online]. Available: *electro.physics.auburn.edu/~park/RESEARCH_2/M... (No date)*

20. M. Egashira, N. Kanehara, Y. Shimizu and H. Iwanaga. *Sensors and Actuators*. 1989, 349-360: 18.

21. N. Hongsith, S. Choopun, P. Mangkorntong and N. Mangkorntong. *J. CMU. Inter.* 2005, 15-20:4.

22. S. Choopun, N. Hongsith, S. Tanunchai, T. Chairuangsri, C. Krua-in, S. Singkarat, T. Vilathong, P. Mangkorntong and N. Mangkorntong. *J. Cryst Growth*. 2005, 365-369:282(3-4).

23. M. C. Newton and P. A. Warburton. *Materialstoday*. 2007, 50-54:10(5).

24. Z. Zhou, H. Deng, J. Yi and S. Liu. *Materials Research Bulletin*. 1999, 1563-1567:34.

25. Y.S. Chang and J.M. Ting. *Thin Solid Films*. 2001, 29- 34: 398- 399.

26. Y.S. Wang, C. Yuen, S.P. Lau, S.F. Yu and B.K. Tay. *Chem. Phys. Lett.*. 2003, 329- 332: 377.

27. X. Kong and Y. Li. *Chemistry Letters*. 2003, 838-839: 32.

28. H. Yuan and Y. Zhang. *J. Cryst. Growth*. 2004, 119- 124: 263.

29. H. Hou, Y. Xiung, Y. Xie, Q. Li, J. Zhang and X. Tian. *Journal of Solid State Chemistry*. 2004, 176- 180: 177.

30. O. A. Lyapina, A. N. Baranov, G. N. Panin, A. V. Knotko, and O. V. Kononenko. *Inorg. Mater.* 2008, 958-965: 8.

31. "---" [online] available *http://www.hokudai.ac.jp/.../H12_08/buturi/topics.html (No date).*

32. S.J. Pearton, D.P. Norton, K. Ip, Y.W. Heo, and T. Steiner. *Superlattices and Microstructures.* 2003, 3-32: 34.

33. S. Choopun, N. Hongsith, E. Wongrat, T. Kamwanna, S. Singkarat, P. Mangkorntong and N. Mangkorntong. *J. Am. Ceram. Soc.*, 2008, 147–177: 91.

34. Z. R. Dai, Z. W. Pan, and Z. L. Wang. *Adv. Funct. Mater.*, 2003, 9-24:13.

35. K. Kongjai, S. Choopun, N. Hongsith and A. Gardchareon. *Chiang Mai J. Sci.*, 2011, 39-46: 38(1).

36. F. K. Shan, B. I. Kim, G. X. Liu, J. Y. Sohn, W. J. Lee, B. C. Shin, and Y. S. Yu. *Appl. Phys.*, 2004, 4772-4776:95.

37. K. L. Chopra, S. major, and D. K. Pandaya. *Thin Solid Films.*, 1983, 1-46:102.

38. ชาญชัย วิริยะวรสกุล "เส้นลวดนาโนซิงค์ออกไซด์โดยการออกซิเดชันของผงสังกะสีเพื่อใช้ เป็นเซนเซอร์เอทานอล" วิทยาศาสตรมหาบัณฑิต สาขาวิชาฟิสิกส์ประยุกต์ มหาวิทยาลัยเชียงใหม่ พ.ศ. 2549.

39. University of the Western Cape, South Africa and Arizona State University, USA "Scanning Electron Microscope (SEM)" [Online]. Available *http://ion.eas.asu.edu/descript_sem.htm (1 October 2004).*

40. วิรุพห์ มังคละวิรัช และ สุวิทย์ ปุฌณชัยยะ "วารสารศูนย์เครื่องมือวิจัยวิทยาศาสตร์และ เทคโนโลยี", 2534, 131: 1(2).

41. ศุภสโรส หมื่นสิทธิ์, วัสดุศาสตร์เชิงฟิสิกส์ , กรุงเทพ; ศูนย์ส่งเสริมกรุงเทพ, 2538, 81-82.

42. R. M.Myers and J.F.Hanlan "The Compositional Analysis of French-Canadian Church Silver" [Online]. *Available. http://collections.ic.gc.ca/bulletin/ num21/myers1_image5.html, (1 October 2004).*

43. R. Jenkins, R.W. Gould, G. Dale. "Quantitative x-ray spectrometry". *New York: Marcel Dekker.,* 1981, 19-20.

44. "Chemistry: Webelement Periodic Table" [online] available
    http://www.webelements.com/webelements/elements/ text/Au/xtal.html
    (No date).

45. B.P. Zhang, N.T. Binh, Y. Segawa, K. Wakatsuki and N. Usami. *Appl. Phys. Lett.*,
    2003, 1635-1637:83.

46. M. Haruta. *Chem. Rec.*, 2000,75–87: 3(2).

47. M. Haruta. *Catal. Surveys Jpn.*, 1997, 61–73:1.

48. G. Neri, A. Bonavita, C. Milone and S. Galvagno. *Sens. Actuators B.*, 2003,
    402–408:93.

49. A. Cho. "Connecting the Dots to Custom Catalysts" *Science.*, 2003,
    1684–1685:299.

50. G. Wang, W. Zhang, H. Lian, Q. Liu, D. Jiang and T. Wu.
    React. Kinet. Catal. Lett., 2002, 343 – 351:75.

51. อัฐสิษฐ์ ทับทิมแท้ "เซนเซอร์เอทานอลที่มีโครงสร้างนาโนซิงก์ออกไซด์เจือด้วยทองคำ
    เป็นฐาน" วิทยาศาสตรมหาบัณฑิต สาขาวิชาฟิสิกส์ประยุกต์ มหาวิทยาลัยเชียงใหม่
    พ.ศ. 2550.

52. S. A. Akbar and P.K. Dutta. "Ceramic Sensor for Industrial Application",
    NFS Center of Industrial Sensor and Measurement Ohio Univ., Columbus.
    2000.

53. N. Hongsith, E. Wongrat, T. Kerdcharoen and S. Choopun. *Sens. Actuators B.*,
    2010, 67-72:144.

ภาคผนวก

ภาคผนวก ก

เทคนิคการเตรียมสารละลายเอทานอลที่ความเข้มข้นต่างๆ [51]

ในงานวิจัยนี้ใช้ความเข้มข้นของไอเอทานอลในหน่วย ppm (part per million) หมายถึง
ความเข้มข้นของไอเอทานอล 1 หน่วย ต่อ อากาศ 1 ล้านหน่วย การเตรียมส่วนผสมสารละลายเอทา
นอลในสถานะก๊าซทำได้ยาก จึงนิยมเตรียมสารละลายเอทานอลให้อยู่ในสถานะของสารละลาย
ความเข้มข้นค่าหนึ่ง โดยอาศัยกฎของเฮนรี (Henry's law) ในการเตรียมสารละลายเอทานอลที่
กล่าวว่า แอลกอฮอล์ในน้ำจะเปลี่ยนแอลกอฮอล์ในอากาศโดยอาศัยค่าสัดส่วน $k_{w/a}$ ซึ่งมี
ความสัมพันธ์ดังสมการ

$$k_{w/a} = \frac{1x10^3}{0.04145e^{0.06583T(^{\circ}C)}}$$
(ก-1)

เมื่อ $k_{w/a}$ คือ สัมประสิทธิ์การแปลงปริมาณแอลกอฮอล์ในน้ำเป็นปริมาณแอลกอฮอล์
ในอากาศ (water-alcohol to air-alcohol partition ratio)

T (°C) คือ อุณหภูมิ หน่วยองศาเซลเซียส (°C)

นอกจากนี้การเปลี่ยนหน่วยจาก ppm เป็น mg/m³ เพื่อใช้ในการเตรียมสารละลายเอทานอล
สามารถเปลี่ยนหน่วยได้จากสมการ

$$1ppm = mg/m^3 = \frac{(ppmv)(12.187)(MW)}{273.15 + T(^{\circ}C)}$$
(ก-2)

เมื่อ mg/m^3 คือ ความเข้มข้นของเอทานอลในน้ำ

$ppmv$ คือ ความเข้มข้นของไอเอทานอลในอากาศ

MW คือ molecular weight

การคำนวณ

ในงานวิจัยนี้ใช้ alcohol simulator ที่ควบคุมอุณหภูมิของสารละลายเอทานอลในน้ำให้มี
อุณหภูมิเท่ากับ 34 องศาเซลเซียส เมื่อนำไปคำนวณค่า $k_{w/a}$ จะได้

$$k_{w/a} = \frac{1x10^3}{0.04145e^{0.06583(34)}} = 2572.935$$

จากค่าคำนวณที่ได้แสดงว่าสารละลายเอทานอล 2573 ส่วน จะระเหยกลายเป็นไอของเอทานอล 1
ส่วน ที่อุณหภูมิ 34 องศาเซลเซียส จากนั้นกำหนดค่าความเข้มข้นของไอเอทานอลเพื่อคำนวณหา
ปริมาณสารละลายเอทานอลในน้ำจากสมการ (ก.2) เช่น ต้องการเตรียมสารละลายเอทานอลให้ได้
ความเข้มข้นของไอเอทานอล 1000 ppm จะคำนวณได้ดังนี้

$$1ppm = mg/m^3 = \frac{(1000)(12.187)(46.07)}{273.15+34} = 1827.9508$$

ปริมาณเอทานอลในน้ำ	=	1827.9508 mg/ m³ จะได้ไอเอทานอล 1 ส่วน
ปริมาณเอทานอลในน้ำทั้งหมด	=	1827.9508 mg/ m³ x 2573
	=	4.7032 x 10⁶ mg/ m³
	=	4.7032 mg/ cm³

เมื่อเตรียมสารละลายเอทานอล 500 มิลลิลิตร จะใช้ปริมาณเอทานอลเท่ากับ 2.3516 กรัม
หมายความว่า จะต้องใช้เอทานอล 2.3516 กรัม ผสมกับน้ำปริมาณ 500 มิลลิลิตร จึงจะได้
สารละลายเอทานอลความเข้มข้น 1000 ppm

ผลการทดสอบสมบัติการตรวจจับไอเอทานอล

ตาราง ข-1 ผลการทดสอบไอเอทานอลที่ความเข้มข้นและอุณหภูมิต่างๆ ของเอทานอลเซนเซอร์ที่ สร้างจาก W-ZnO

อุณหภูมิ (°C)	สารละลาย เอทานอล (ppm)	R_{air} (Ω)	R_{gas} (Ω)	sensitivity (R_{air}/R_{gas})	response time (s)	recovery time (s)
100	1000	30012	29402	1.021	136.66	185.56
	500	30323	29756	1.019	85.10	126.10
	100	29928	29746	1.006	30.70	91.00
	50	30146	29769	1.013	61.64	55.96
120	1000	30803	30477	1.011	165.29	214.18
	500	30997	30682	1.010	189.85	283.89
	100	31099	30804	1.010	148.77	172.47
	50	31236	30827	1.013	155.85	283.88
140	1000	30540	30013	1.018	98.73	105.01
	500	30249	30062	1.006	46.40	42.99
	100	30470	30286	1.006	36.76	22.73
	50	30708	30499	1.007	36.75	41.69
160	1000	29164	28821	1.012	19.38	8.46
	500	29403	28672	1.025	54.35	38.98
	100	29458	29167	1.010	21.55	11.44
	50	29627	29304	1.011	21.26	12.18
180	1000	28102	27714	1.014	14.83	16.18
	500	28132	27717	1.015	17.71	15.15
	100	28307	27703	1.022	32.34	31.41
	50	27359	27263	1.004	9.44	446.68
200	1000	26551	25836	1.028	71.25	46.05
	500	26618	26105	1.020	33.75	32.03
	100	26635	26069	1.022	26.89	40.86
	50	26758	26217	1.021	22.01	22.80

อุณหภูมิ (°C)	สารละลายเอทานอล (ppm)	R_{air} (Ω)	R_{gas} (Ω)	sensitivity (R_{air}/R_{gas})	response time (s)	recovery time (s)
220	1000	24002	23389	1.026	8.27	46.01
	500	24029	23455	1.024	10.03	197.86
	100	24036	23652	1.016	8.47	27.79
	50	24002	23601	1.017	10.97	9.25
240	1000	22826.22	21379.34	1.068	34.60	72.98
	500	22842.58	21818.3	1.047	12.09	53.72
	100	22835.54	22009.13	1.038	13.18	39.46
	50	23054.46	22156.02	1.041	7.61	27.82
260	1000	22658.34	20281.05	1.117	17.88	90.30
	500	22525.2	20247.67	1.112	38.37	62.49
	100	22568.37	21313.58	1.059	12.10	29.33
	50	22600.37	20865.28	1.083	13.17	40.55
280	1000	21812.01	18683.24	1.167	108.87	89.00
	500	21816.61	19041.98	1.146	15.45	63.77
	100	22335.73	20197.57	1.106	12.99	51.03
	50	22510.57	20260.29	1.111	6.08	50.59
300	1000	21585.65	17225.59	1.253	11.81	69.31
	500	21610.13	17711.83	1.220	10.03	64.56
	100	21504.91	18729.78	1.148	10.13	42.21
	50	21661.04	18551.07	1.168	5.02	40.53
320	1000	20608	15912	1.295	7.59	50.37
	500	20615.36	16273.92	1.267	11.00	41.69
	100	20559.32	17565.8	1.170	13.16	31.34
	50	20855.11	17179.89	1.214	8.26	30.72

อุณหภูมิ (°C)	สารละลาย เอทานอล (ppm)	R_{air} (Ω)	R_{gas} (Ω)	sensitivity (R_{air}/R_{gas})	response time (s)	recovery time (s)
340	1000	18917	13814	1.369	11.41	37.31
	500	19081.99	14900.51	1.281	55.14	25.42
	100	19330.97	16451.32	1.175	9.58	18.54
	50	19383.98	16627.24	1.166	10.31	17.02
360	1000	18263	13351	1.368	6.88	33.41
	500	18026.95	13229.79	1.363	23.88	46.19
	100	18030.47	15407.04	1.170	16.17	12.88
	50	17869.81	15862.67	1.127	8.50	9.08
380	1000	17944	14102	1.272	8.97	37.85
	500	17885.47	14763.6	1.211	4.68	34.23
	100	17635.09	15336.39	1.150	8.10	22.90
	50	17455.41	14886.24	1.173	7.35	22.90

ตาราง ข-2 ผลการทดสอบไอเอทานอลที่ความเข้มข้นและอุณหภูมิต่างๆ ของเอทานอลเซนเซอร์ที่สร้างจาก *W*-ZnO เจือด้วยอนุภาคนาโนของทองคำ 0.1%mol

อุณหภูมิ (°C)	สารละลายเอทานอล (ppm)	R_{air} (Ω)	R_{gas} (Ω)	sensitivity (R_{air}/R_{gas})	response time (s)	recovery time (s)
100	1000	47184.13	46937.28	1.005	195.70	323.90
	500	47202.83	46947.97	1.005	168.68	284.78
	100	47314.22	46988.7	1.007	205.12	337.43
	50	47308.29	47029.81	1.006	234.88	429.21
120	1000	47918.96	47360.06	1.012	170.41	244.59
	500	47929.19	47407.25	1.011	152.55	211.89
	100	47671.1	47252.89	1.009	163.33	193.00
	50	46962.06	46721.5	1.005	172.78	209.22
140	1000	47914.32	47402.89	1.011	129.90	84.99
	500	47699.55	47214.6	1.010	112.01	71.55
	100	48150.46	47806.45	1.007	102.56	40.54
	50	48097.76	47685.13	1.009	78.32	60.68
160	1000	43350.42	42596.17	1.018	117.64	58.49
	500	43343.35	42653.32	1.016	102.57	44.55
	100	43617.66	43217.76	1.009	54.00	44.55
	50	43461.12	42843.17	1.014	55.34	41.88
180	1000	37929.97	36508.1	1.039	107.87	63.76
	500	38062.03	36903.2	1.031	101.22	51.24
	100	38133.79	37569.32	1.015	39.20	33.68
	50	38594.99	37801.05	1.021	40.46	24.32
200	1000	33335.59	31463.87	1.059	89.52	78.89
	500	33296.47	31863.95	1.045	90.45	58.02
	100	33417.88	32784.59	1.019	66.20	31.01
	50	33479.26	33031.03	1.014	28.42	18.89

อุณหภูมิ (°C)	สารละลายเอทานอล (ppm)	R_{air} (Ω)	R_{gas} (Ω)	sensitivity (R_{air}/R_{gas})	response time (s)	recovery time (s)
220	1000	30287.96	27787.97	1.090	53.13	104.75
	500	30207.23	28174.76	1.072	76.90	75.56
	100	29828.93	28758.81	1.037	39.20	40.54
	50	30033.85	28843.28	1.041	32.43	37.78
240	1000	27635.28	24906.19	1.110	56.67	73.11
	500	27427.61	25118.07	1.092	56.67	67.46
	100	27435.67	25966.87	1.057	22.98	40.46
	50	27515.85	25947.29	1.060	18.89	41.79
260	1000	25368.17	22433.26	1.131	13.24	62.72
	500	25253.73	22694.37	1.113	12.12	56.67
	100	25280.53	23584.74	1.072	9.45	28.33
	50	25195.18	23508.84	1.072	8.11	29.67
280	1000	24292.41	20842.27	1.166	18.69	59.94
	500	24184.91	21317.96	1.134	9.45	52.66
	100	24177.4	22338.18	1.082	10.87	29.67
	50	24267.09	22234.09	1.091	6.77	27.00
300	1000	22957.77	19231.66	1.194	17.46	41.48
	500	22825.57	19762.42	1.155	14.88	35.02
	100	22792.77	20755.56	1.098	10.78	24.24
	50	22870.38	20721.41	1.104	8.11	20.22
320	1000	21530.94	17733.33	1.214	8.56	22.43
	500	21513.52	18396.7	1.169	8.11	21.65
	100	21483.87	19464.53	1.104	8.11	14.80
	50	21550.7	19468.98	1.107	10.79	16.21

อุณหภูมิ (°C)	สารละลาย เอทานอล (ppm)	R_{air} (Ω)	R_{gas} (Ω)	sensitivity (R_{air}/R_{gas})	response time (s)	recovery time (s)
340	1000	20158.24	16306.1	1.236	4.80	15.36
	500	20117.54	16704.82	1.204	5.50	11.32
	100	19896.39	17760.77	1.120	5.32	9.06
	50	19804.84	18264.85	1.084	5.40	5.80
360	1000	18812.37	15607.42	1.205	4.09	12.83
	500	18675.9	15896.85	1.175	4.01	13.46
	100	18266.96	16592.95	1.101	4.01	10.78
	50	18317.27	16765.95	1.093	4.09	6.77

การตรวจสอบโครงสร้างทางผลึกด้วย XRD เทียบกับฐานข้อมูล JCPDS

การตรวจสอบโครงสร้างทางผลึกของ ZnO whiskers ที่นำมาประยุกต์ใช้เป็นเอทานอล เซนเซอร์ในงานวิจัยนี้ด้วย XRD พบว่ามีโครงสร้างแบบเฮกซะโกนอล (hexagonal structure) และวิเคราะห์ค่า lattice constant ของโครงสร้างจากสมการ

$$\frac{1}{d_{hkl}^2} = \frac{4}{3}\left(\frac{h^2 + hk + k^2}{a^2}\right) + \frac{l^2}{c^2} \qquad \text{(ค-1)}$$

พบว่า โครงสร้าง T-ZnO และ W-ZnO ที่สังเคราะห์ได้เมื่อเทียบกับฐานข้อมูล JCPDS หมายเลข 89-0510 ดังตาราง ค-1 และรูป ค-1 ตรงกับระนาบ (100) (002) (101) (102) (110) (103) (200) (112) (201) (004) และ (202) ตามลำดับ โดยมีค่า lattice constant ดังแสดงในตารางที่ 4.5-4.7

ตารางที่ ค-1 ผลการเปรียบเทียบระยะห่างระหว่างระนาบ (d_{hkl}) ของ T-ZnO กับฐานข้อมูล JCPDS no. 89-0510

สาร	d_{hkl}	d_{hkl} จากการทดลอง	d_{hkl} จาก JCPDS no. 89-0510	%error; < 3.5%
T-ZnO	d_{100}	2.7884	2.8135	0.8921
	d_{002}	2.5814	2.6027	0.8184
	d_{101}	2.4563	2.4751	0.7596
	d_{102}	1.9012	1.9105	0.4868
	d_{110}	1.6187	1.6244	0.3509
	d_{103}	1.4725	1.4768	0.2912
	d_{200}	1.4030	1.4067	0.2630
	d_{112}	1.3743	1.3780	0.2685
	d_{201}	1.3546	1.3580	0.2504
	d_{202}	1.2348	1.2375	0.2182

ตารางที่ ค-2 ผลการเปรียบเทียบระยะห่างระหว่างระนาบ (d_{hkl}) ของ W-ZnO กับฐานข้อมูล JCPDS no. 89-0510

สาร	d_{hkl}	d_{hkl} จากการทดลอง	d_{hkl} จาก JCPDS no. 89-0510	%error; < 3.5%
	d_{100}	2.7889	2.8135	0.8744
	d_{002}	2.5805	2.6027	0.8530
	d_{101}	2.4575	2.4751	0.7111
	d_{102}	1.9010	1.9105	0.4973
W-ZnO	d_{110}	1.6224	1.6244	0.1231
	d_{103}	1.4722	1.4768	0.3115
	d_{200}	1.4014	1.4067	0.3768
	d_{112}	1.3740	1.3780	0.2903
	d_{201}	1.3540	1.3580	0.2946
	d_{004}	1.2981	1.3013	0.2459

ตารางที่ ค-3 ผลการเปรียบเทียบระยะห่างระหว่างระนาบ (d_{hkl}) ของ W-ZnO ที่เจือด้วยอนุภาคนาโนของทองคำ 0.1%mol กับฐานข้อมูล JCPDS no. 89-0510

สาร	d_{hkl}	d_{hkl} จากการทดลอง	d_{hkl} จาก JCPDS no. 89-0510	%error; < 3.5%
	d_{100}	2.7973	2.8135	0.5758
	d_{002}	2.5874	2.6027	0.5879
	d_{101}	2.4620	2.4751	0.5293
	d_{102}	1.9040	1.9105	0.3402
	d_{110}	1.6206	1.6244	0.2339
W-ZnO	d_{103}	1.4743	1.4768	0.1693
	d_{200}	1.4028	1.4067	0.2772
	d_{112}	1.3756	1.3780	0.1742
	d_{201}	1.3560	1.3580	0.1473
	d_{004}	1.2994	1.3013	0.1460
	d_{202}	1.2356	1.2375	0.1535

PDF # 890510, Wavelength = 1.54060 (A)   _ □ ×

89-0510	Quality: C

CAS Number:

| Molecular Weight: 81.38 |
| Volume[CD]: 47.58 |
| Dx: 5.680   Dm: |

| Sys: Hexagonal |
| Lattice: Primitive |
| S.G.: P63mc (186) |
| Cell Parameters: |
| a 3.248   b   c 5.205 |
| α   β   γ |

| I/Icor: 5.38 |
| Rad: CuKa1 |
| Lambda: 1.54060 |
| Filter: |
| d-sp: calculated |
| ICSD # : 082028 |

Zn O
Zinc Oxide
Ref: Calculated from ICSD using POWD-12++
Ref: Sawada, H., Wang, R., Sleight, A.W., J. Solid State Chem., 122, 148 (1996)
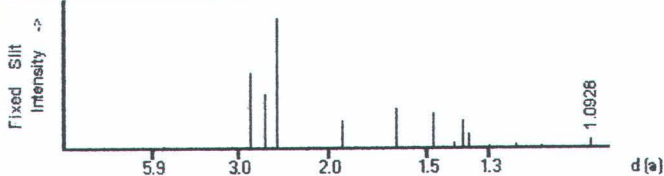
d(A)	Int-f	h	k	l	d(A)	Int-f	h	k	l	d(A)	Int-f	h	k	l
2.8135	570	1	0	0	1.4768	264	1	0	3	1.2375	32	2	0	2
2.6027	414	0	0	2	1.4067	40	2	0	0	1.1811	16	1	0	4
2.4751	999 *	1	0	1	1.3780	214	1	1	2	1.0927	65	2	0	3
1.9105	210	1	0	2	1.3580	105	2	0	1					
1.6244	301	1	1	0	1.3013	16	0	0	4					

PDF # 890510, Wavelength = 1.54060 (A)   _ □ ×

89-0510	Quality: C

CAS Number:

| Molecular Weight: 81.38 |
| Volume[CD]: 47.58 |
| Dx: 5.680   Dm: |

| Sys: Hexagonal |
| Lattice: Primitive |
| S.G.: P63mc (186) |
| Cell Parameters: |
| a 3.248   b   c 5.205 |
| α   β   γ |

| I/Icor: 5.38 |
| Rad: CuKa1 |
| Lambda: 1.54060 |
| Filter: |
| d-sp: calculated |
| ICSD # : 082028 |

Zn O
Zinc Oxide
Ref: Calculated from ICSD using POWD-12++
Ref: Sawada, H., Wang, R., Sleight, A.W., J. Solid State Chem., 122, 148 (1996)
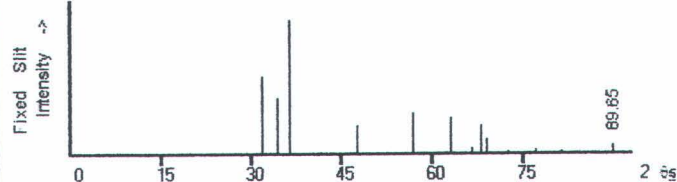
2θ	Int-f	h	k	l	2θ	Int-f	h	k	l	2θ	Int-f	h	k	l
31.779	570	1	0	0	62.876	264	1	0	3	76.988	32	2	0	2
34.430	414	0	0	2	66.400	40	2	0	0	81.411	16	1	0	4
36.265	999 *	1	0	1	67.971	214	1	1	2	89.646	65	2	0	3
47.554	210	1	0	2	69.112	105	2	0	1					
56.615	301	1	1	0	72.587	16	0	0	4					

รูปที่ ค-1 ฐานข้อมูล JCPDS no. 89-0510

ภาคผนวก ง

ผลงานทางวิชาการ

1. การนำเสนอผลงาน

1.1 นำเสนอผลงานในรูปแบบโปสเตอร์ในการประชุมวิชาการระดับชาติ

"THE FIRST THAILAND NATIONAL NANOTECHNOLOGY CONFERENCE ON NANOMATERIALS, PHARMACEUTICALS, DEVICES AND APPLICATIONS " Held at Daung Tawan Grand Ballroom, Central Daung Tawan Hotel in Chiang Mai, Thailand, from 14-16 August 2007. The Conference was organized by Network for the Excellence in Functional Nanomaterials (NEFNC), Chiang Mai University and National Nanotechnology Center (NANOTEC).

2.2 นำเสนอผลงานแบบบรรยาย (oral presentation) ในการประชุมวิชาการระดับนานาชาติ

"German-Thai Symposium on Nanoscience and Nanotechnology 2009"

จัดโดย สถานเอกอัครราชทูตไทย ณ กรุงเบอร์ลินสหพันธ์สาธารณรัฐเยอรมันนีร่วมกับคณะวิทยาศาสตร์ มหาวิทยาลัยเชียงใหม่ และคณะวิทยาศาสตร์ มหาวิทยาลัยเกษตรศาสตร์ ระหว่างวันที่ 21-22 กันยายน พ.ศ. 2552 ณ โรงแรมเชียงใหม่ออร์คิด จังหวัดเชียงใหม่

2. ผลงานตีพิมพ์

2.1 ชื่อเรื่อง: Preparation of Zinc Oxide Nanostructures by Thermal Oxidation of Zinc: Zinc Oxide: Carbon Mixtures.

ชื่อผู้แต่ง: Kiattipoom Kongjai, Dusadee Srisongrach, Nikorn Mangkorntong, Pongsri Mangkorntong and Supab Choopun

ชื่อวารสาร: CUM. J. Nat. Sci. Special issue on Nanotechnology ฉบับที่ 7(1) ปีที่ 2008 หน้าที่ 37-41

2.2 ชื่อเรื่อง: Zinc Oxide Whiskers by Thermal Oxidation Method.

ชื่อผู้แต่ง: Kiattipoom Kongjai, Supab Choopun, Niyom Hongsith and Atcharawon Gardchareon.

ชื่อวารสาร: Chiang Mai J. sci ฉบับที่ 38(1) ปีที่ 2011 หน้าที่ 39-46

Preparation of Zinc Oxide Nanostructures by Thermal Oxidation of Zinc:Zinc Oxide:Carbon Mixtures

Kiattipoom Kongjai, Dusadee Srisongrach, Nikorn Mangkorntong, Pongsri Mangkorntong and Supab Choopun*

Department of Physics, Faculty of Science, Chiang Mai University, Chiang Mai 50200, Thailand

*Corresponding author. E-mail: supab@science.cmu.ac.th

ABSTRACT

Zinc oxide nanostructures were prepared by thermal oxidation of zinc, zinc oxide and carbon mixtures. The mixture was screened on the alumina substrate and heated at 800°C for 1 hour under normal atmosphere. The influence of the mixture ratio on the formation of nanostructure was investigated with field emission scanning electron microscope and an energy dispersive spectroscope. It was found that the size of nanostructures depended on the ratio of the mixture. The higher ZnO:Zn ratio led to the formation of shorter, and less density of nanostructure. However, there was a number ratios with carbon that could form long and high density of nanostructure.

Key words: Zinc oxide, Nanostructure, Nanowire, Nanobelt

INTRODUCTION

Zinc oxide is a metal oxide wide-band gap semiconductor (Christoulakis et al., 2006) which has been widely studied. These include the fabrication of nanodevices (Wang et al., 2006) and various applications, such as gas sensors (Nanto et al., 1996), piezoelectric devices (Gardeniers et al., 1998), varistors (Miguel et al., 2006), planar optical waveguides (Wenas et al., 1991), transparent electrodes (Kim et al., 1997), ultraviolet photodetectors, surface acoustic wave devices. Zinc oxide nanostructures could be synthesized by several techniques such as vapor deposition, sputtering, pulsed laser deposition (PLD), oxidation and screen printing (silk screen). Screen printing has been developed in the fields of microelectronics for hybrid and integrated circuit manufactures (Miguel et al., 2006) and this technique is well known as one of most important thick film deposition methods (Ivanov, 2004). The advantages of this method are simple, low cost, fast and high reproducibility.

In this work, zinc oxide nanostructures were synthesized by thermal oxidation using screen printing of zinc, zinc oxide and carbon mixtures. The effect of the mixture ratio on the formation of nanostructures was investigated.

MATERIALS AND METHODS

Zinc oxide nanostructures were prepared by thermal oxidation technique. The starting materials, zinc (Zn), zinc oxide (ZnO) and carbon (C) powders were mixed in the various ratio by molar of Zn: ZnO: C with 1:0:0, 2:1:0, 1:1:0, 1:2:0, 2:0:1, 1:0:1, 1:0:2, 4:2:3, 4:2:2 and 4:3:2. The mixed powders were hand-grounded in agate mortar with polyvinyl alcohol (PVA). After that, the mixture was screened on alumina substrate and heated under atmosphere at 800?C for 1 hour. Zinc oxide nanostructures were characterized by Field-Emission Scanning Electron Microscopy (FE-SEM) for morphology and energy dispersive spectroscopy (EDS) for chemical composition. From SEM images, we used computer program (Image J) to carry out density of nanostructures by fixed area of 25 μm^2 (number of nanostructure/25 μm^2) for 5 times per condition, then the average value of density of nanostructures were obtained.

RESULTS AND DISCUSSION

Before heating, the color of starting materials are gray and black depending on the amount of zinc and carbon powders since typical color of zinc and carbon are black respectively. After heating, zinc was oxidized with oxygen in normal atmosphere and transformed to zinc oxide and thus, the color of thick films changed from black or gray to yellow or white which is the typical color of zinc oxide. The morphology of zinc oxide nanostructures grown on alumina substrates at various Zn: ZnO: C ratio was shown in Figure 1. The wire-like nanostructures were observed only at the ratio of 1:0:1(Figure 1(b)). For the other ratios, the belt-like nanostructures were observed.

Table 1. The color of ZnO nanostructures before and after heating.

Type of films	Color before heating	Color after heating
Zn : ZnO	gray	yellow + white
Zn : C	black	yellow + white
Zn : ZnO : C	black	yellow + white

The colors of ZnO nanostructures were toned to change after heating under atmosphere at 800°C for 1 hour as listed in Table 1.
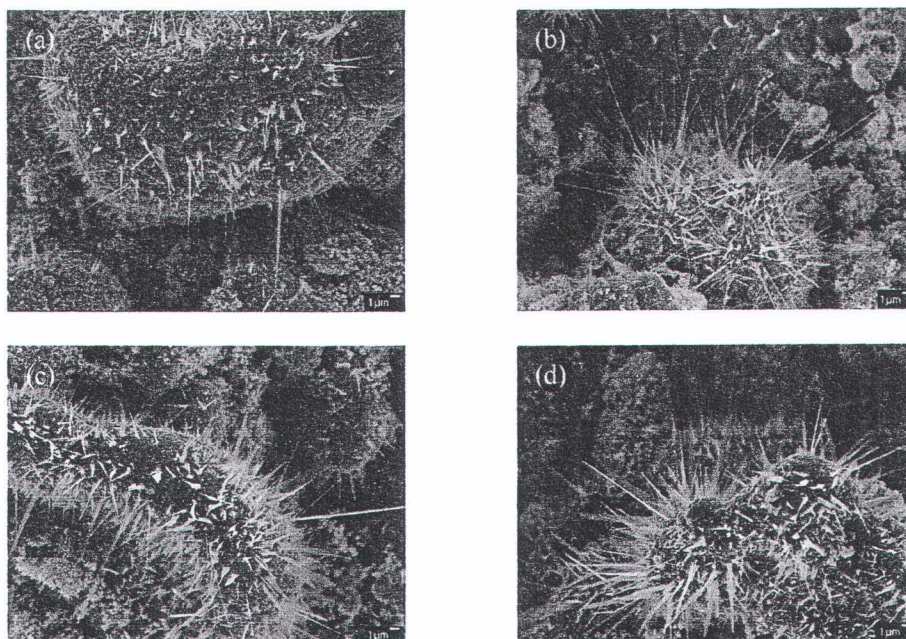
Figure 1. FE-SEM images of thick films with various Zn: ZnO: C ratio of (a) 2: 1:0, (b) 1:0:1, (c) 4:2:3, (d) 4:2:2.

The length and density of zinc oxide nanostructures at different ratios were shown in Table 2. The length and density of zinc oxide nanostructures depended on the Zn: ZnO: C ratio. The higher ZnO:Zn ratio led to the formation of shorter, and less density of nanostructures. However, there was a number ratios with carbon that could form long and high density of zinc oxide nanostructures.

Table 2. The length and density of zinc oxide nanostructures at different Zn: ZnO: C ratio.

Zn: ZnO: C ratio	Type of ZnO nanostructure	Average length (μm)	Density (number of nanostructures/25μm²)
1:0:0	Belt	2.96	6
2:1:0	Belt	5.16	20
1:1:0	Belt	2.23	8
1:2:0	Belt	1.90	5
2:0:1	Belt	4.85	9
1:0:1	Wire	20.73	18
1:0:2	Belt	4.64	15
4:2:3	Belt	4.84	9
4:2:2	Belt	6.92	20
4:3:2	Belt	6.24	8

Figure 2 showed EDS spectra of (a) zinc oxide nanowire and (b) zinc oxide nanobelt. The spectra were obtained by focusing electron beam in a middle of nanostructures. The peaks at Zn and O signals were observed indicating Zn was oxidized with O and formed zinc oxide nanostructures. The atomic ratio of zinc and oxygen from the EDS spectra of nanowire and nanobelt were 39:61 and 47:53, respectively, which was nearly 1:1 ratio. Thus, the obtained nanostructures could be considered as ZnO.
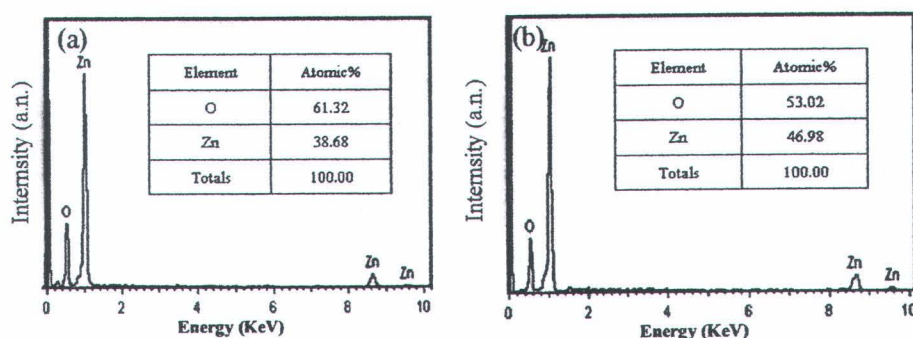
Figure 2. EDS spectra of (a) ZnO nanowires and (b) ZnO nanobelts.

CONCLUSION

The zinc oxide nanostructures were successfully synthesized by thermal oxidation of zinc, zinc oxide and carbon mixture with various Zn: ZnO: C ratios. From FE-SEM analysis, it was found that the size of nanostructures depended on the ratio of the mixture. The higher ZnO:Zn ratio led to the formation of shorter, and less density of nanostructure. However, there was a number ratios with carbon that could form long and high density of nanostructure.

ACKNOWLEGEMENTS

REFERENCES

Christoulakis, S., M. Suchea, E. Koudoumas, M. Katharakis, N. Katsarakis, and G. Kiriakidis. 2006. Thickness influence on surface morphology and ozone sensing properties of nanostructured ZnO transparent thin films grown by PLD. Appl. Surf. Sci. 252: 5351-5354.

106

Gardeniers, J. G. E., Z. M. Rittersma, and G. J. Burger. 1998. Preferred orientation and piezoelectricity in sputtered ZnO films. J. Appl. Phys. 83: 7844-7854.

Ivanov, P. T. 2004. Design, fabrication and characterization of thick-film gas sensors. Engineerng Electronics. Ph.D. Dissertation. Rovira I Virgili university. Spain.

Kim, K. H., K. C. Park, and D. Y. Ma. 1997. Structural, electrical and optical propertiesof aluminum doped zinc oxide films prepared by radio frequency magnetron Sputtering. J. Appl. Phys. 81: 7764-7772.

Miguel, Angel de la Rubia Lopez., M. Peiteado , J. F. Fernandez , A. C. Caballero, J. Holc, S. Drnovsek, D. Kuscer, S. Macekb, and M. Kosec. 2006. Thick film ZnO based varistors prepared by screen printing. J. Euro. Ceram. Soc. 26: 2985-2989.

Nanto, H., T. Morita, H. Habara, K. Kondo, Y. Douguchi, and T. Minamia. 1996. Doping effect of SnO2 on gas sensing characteristics of sputtered ZnO thin film chemical sensor. Sens. Actuators B. 35-36: 384-387.

Wang, H., C. Xie, D. Zeng and Z. Yang. 2006. Controlled organization of ZnO building blocks into complex nanostructures. J. Colloid Interface Sci. 297: 570-577.

Wenas, W. W., A. Yamada, and K. Takahashi. 1991. Electrical and optical properties of boron-doped ZnO thin films for solar cells grown by metalorganic chemical vapor deposition. J. Appl. Phys. 70: 7119-7123.

Zinc Oxide Whiskers by Thermal Oxidation Method

Kiattipoom Kongjai, Supab Choopun, Niyom Hongsith and Atcharawon Gardchareon*

Department of Physics and Materials Science, Faculty of Science, Chiang Mai University, Chiang Mai 50200, Thailand and ThEP Center, CHE, Bangkok 10400, Thailand.
*Author for correspondence; e-mail: scphi002@chiangmai.ac.th

ABSTRACT

ZnO whiskers were grown in quartz tube by thermal oxidation method. Zinc powder was heated in a horizontal quartz tube with a furnace at a temperature of 700°C for 2 hr, under normal atmosphere. Three different kinds of the products can be obtained after the oxidation process. One is transparent whiskers located at the bottom of the quartz tube. Next is cotton-like bulk and the other is white, fluffy product. The products were characterized by field emission scanning electron microscopy (FE-SEM) and energy dispersive spectroscopy (EDS). It was found that the products composed of whiskers and tetrapod whiskers. The lengths and the diameter of whiskers were in the range of 10-240 mm and 0.20 - 4.60 mm, respectively while the percent of yield was up to 20% by weight. The lengths and the diameter of tetrapod whiskers were in the range of 3.15-10.63 mm and 0.13- 2.64 mm while the percent of yield was up to 68% by weight.

Keywords: zinc oxide, whisker, tetrapod, thermal oxidation.

1. INTRODUCTION

Recently, quasi one-dimensional (1D) nanostructures such as whiskers, wires, rods, belts, and tubes have received the great interest due to their very large surface-to-volume ratio and become the focus of intensive research owing to their unique applications in mesoscopic physics, fabrication of nanoscale optic and electronic devices [1]. ZnO is now receiving special attention for it potential applications in optical and electronic materials [2]. It is an n-type semiconductor with a direct band gap of 3.37 eV at room temperature close in properties to GaN (E_g = 3.5 eV at room temperature), which is widely used in the fabrication of blue light emitting diodes.

The strong exciton binding energy of 60 meV, which is much larger than that of GaN (25 meV) and the thermal energy at room temperature (26 meV) can ensure an efficient exciton emission at room temperature under low excitation energy [2-5]. ZnO can be grown into a variety of micro and nanostructures, such as tetrapod-shape, microrods, one-dimensional microtubes, thin film, nanobelts, nanowires, nanoneedles, nanotubes, nanorods, nanocables and whiskers [1, 6-14]. ZnO nanostuctures are particularly adaptable and have various potential applications, such as gas sensors [15, 16], solar cells [17], field emitters [18] and the field effect

transistor (FET) [19]. Among them, ZnO whisker has attended due to ease of preparation and single crystalline properties.

ZnO whiskers have a hexagonal columnar shape (pencil-like structure) and ZnO whiskers, having tatrapod shape, consist of a ZnO core in the zinc blended structure form in which four ZnO arms in the wurtzite structure radiate. Each arm is well faceted with a hexagonal cross-section and is uniform in length and diameter [20]. Among kinds of ZnO whiskers, tetrapod whisker possesses good comprehensive properties, such as semiconductivity, wear resistance, vibration insulation and microwave absorption. Owing to the unusual geometry and single crystalline character, they can be widely applied as both devices and structural materials [21,22]. In particular, the introduction of ZnO tetapod whiskers imparts antielectrostatic and antibacterial properties to polyacrylate-based composites. Tetrapod-polymer composites can be used in the fabrication of solar cells. Moreover, similarly other structures, ZnO whiskers have attractive gas-sensing and luminescent properties [2].

Due to these promising applications, ZnO whiskers can be prepared by several methods such as solvothermal [1], thermal evaporation [23], Metal Organic Chemical Vapor Deposition (MOCVD) [24], Pulsed Laser Deposition (PLD) [25] and thermal oxidation [15,16,21,22]. The thermal oxidation method is a simple, low cost and fast process. So in this work, ZnO whiskers were prepared with high yield by thermal oxidation of Zn powder.

2. MATERIALS AND METHODS

ZnO whiskers were prepared by thermal oxidation technique. In typical preparation processes, Zn powder mass (Ajax Finechem, quoted purity of 99.9%) was used at weight of 3, 3.5, 4, 4.5, 5, 5.5 and 6 g then the powder

was hand-grounded in agate mortar. After that, ZnO powder was put into the horizontal one-end sealed quartz tube (150 ml) to serve as the source materials. The quartz tube was then pushed into the central of a conventional tube furnace under normal atmosphere at 700°C. The gate of the furnace was closed without special sealing during the whisker generation process. After 2 hr. sintering, the quartz tube was taken out from the furnace into air for rapid cooling.

The obtained products were investigated by field emission scanning electron microscope for morphology and energy dispersive spectroscopy for chemical composition.

3. RESULTS AND DISCUSSION

Before heating, a typical color of zinc powder is grey. After heating process, Zn was oxidized with O_2 in normal atmosphere and transform to ZnO. It was observed that wall of the quartz tubes were covered with a white layer product and there were three different kinds of the products ranging from the bottom to the edge of the quartz tube. One is transparent columned whiskers located at the bottom of the quartz tube. Next is white, cotton-like bulk and other is white, fluffy product. It can be further classified in three portions according to morphologies and density, namely the first portion, the second portion and the third portion as showed in Figure 1.

The different morphologies of products in different portions due to the growth mechanism of the wire-like nanostructures including nanowires, nanorods, nanobelts and whiskers can be explained by the kinetics of anisotropic growth via a vapor-solid mechanism represented as:

$$P = B \exp\left(\frac{-\pi\sigma^2}{k_B^2 T^2 \ln(\alpha)}\right)$$
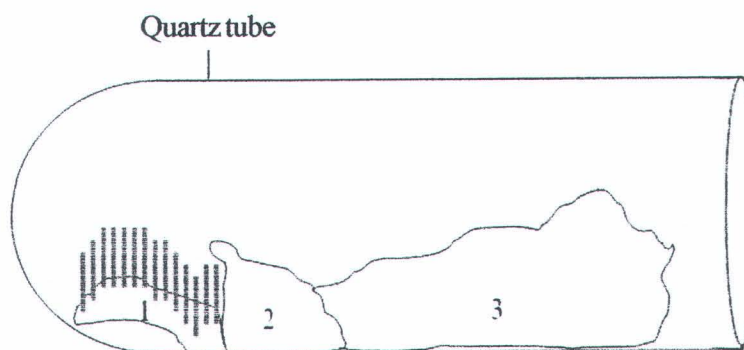
Figure 1. Schematic of the ZnO whiskers formed in different portion in the quartz tube.

where P is the nucleation probability on the surface of a whisker, B is a constant parameter, σ is the surface energy of the solid whisker, k_B is the Boltzmann's constant, T is the absolute temperature, and α is the supersaturation ratio between the actual vapor pressure and the equilibrium vapor pressure corresponding to temperature (usually, > 1) [26-28]. The supersaturation ratio play an important parameter in controlling morphology of wire-like and belt-like nanostructures[26]. Smaller supersaturation ratio promotes the growth of wire-like structures. In contrast, larger supersaturation ratio promotes two dimensional growths resulting in the formation of belt-like structures. However, the tetrapod whisker was not grown on substrate and the supersaturation ratio should be larger than belt-like structures for facilitate the three dimension nucleation resulting in the formation of tetrapod whiskers [28].

In this work Zn in gas phase can be occurred when we heat Zn metal at 700°C which above melting point of it. The mechanism can be explained based on the thermal oxidation reaction which expressed as:

$$2Zn_{(g)} + O_{2(g)} \rightarrow ZnO_{(s)}$$
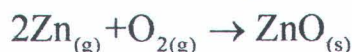
The O_2 for this reaction come from the residual O_2 inside the tube at the beginning and the O_2 which enter into the quartz tube from

the opened end. Then the O_2 concentration near the opened end of the tube is higher than the O_2 concentration far inside the tube therefore the supersaturation ratio of ZnO vapor near the opened end is larger than at the bottom. In this result the shape of products depend on the supersaturation ratio of ZnO vapor's zone in the quartz tube as can see from the SEM images in Figure 2 which the first portion is composed of ZnO whiskers with the hexagonal column (pencil-like structure). The diameter and length were in the range of 30-140 mm and 0.38-4.59 mm, respectively (Figure 2a). The second portion is white and quite dense. It consists of tetrapod whiskers which have the hexagonal cylinder legs. The leg-length of 7.34 ± 0.87 (6.17-9.21) μm and the diameter of 0.32-0.66 (0.49 ± 0.09) μm (Figure 2b). We obtained two types of tetrapod whiskers in the third portion. In this portion, there is the highest concentration of O_2 lead to high probability of Zn vapor oxidized with O_2. Large supersaturation ratio promotes tetrapod growth easily. The obtained tetrapod whiskers have 2 different kinds due to the growthing time. That mean tetrapod whisker in the inner layer have been grown first and the growth is continuously. Thus, the tetrapod whiskers in the inner layer will be longer and bigger than that in the outer layer as showed in the figure that the outer

layer is white, fluffy which quite porous with a thickness of about 1-3 mm and it is composed of tetrapod whiskers which have the leg-length of 4.77 ± 1.46 (3.15-8.87) μm and the diameter of 0.66 ± 0.14 (0.43-0.97) μm at the base, 0.21 ± 0.05 (0.13-0.28) μm at the needle (Figure 2c). The inner layer composed of tetrapod whiskers which have the hexagonal cylinder legs. The leg-length of 7.21 ± 1.64 (4.26-10.63) μm and the diameter of 1.50 ± 0.65 (0.67-2.64) μm (Figure 2d). By SEM observation, the tetrapod whiskers become shorter in leg-length and smaller in aspect ratio as from outside to inside.
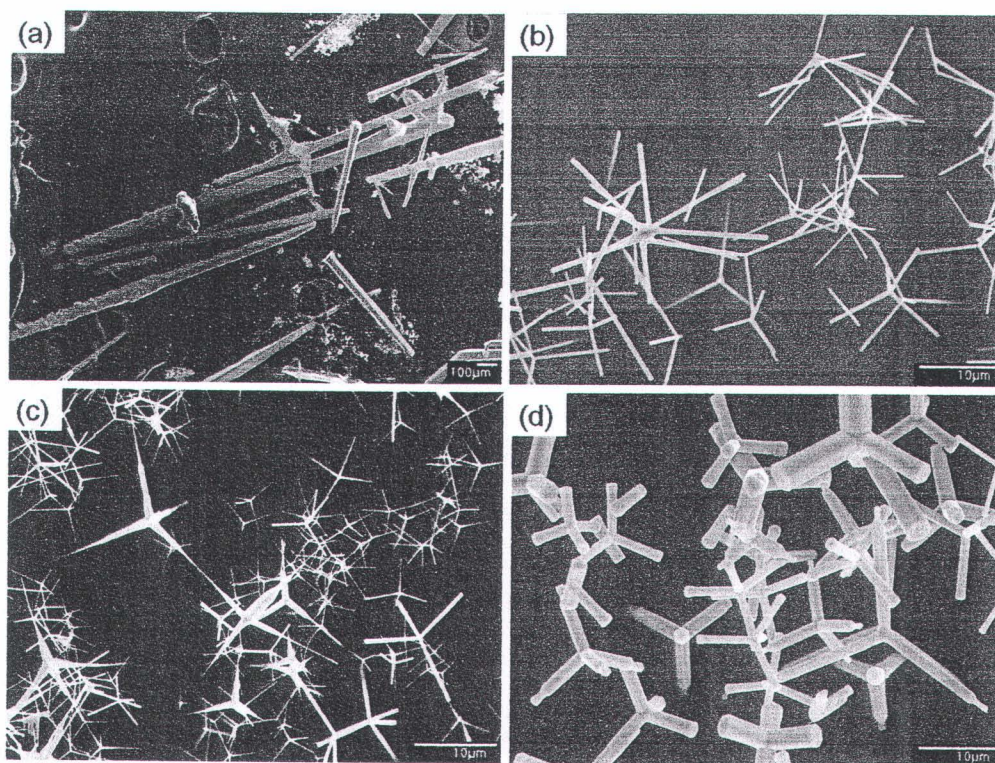
Figure 2. SEM images of ZnO whiskers in difference portions. (a) first portion, (b) second portion, (c) outer layer of third portion, d) inner layer of third portion.

Figure 3 showed EDS spectra of (a) whisker and (b) tetrapod whisker. The spectra were obtained by focusing electron beam in the top of whisker. The peaks at Zn and O signals indicated that Zn was oxidized with O and form ZnO whiskers. The atomic ratio of Zn and O from the EDS spectra of whisker and tetrapod whisker were 47.65 : 52.35 and 44.19 : 55.81, which was nearly 1:1 ratio. Thus, the obtained whisker could be considered as ZnO.

Figure 4 showed the effect of Zn powder weight on the producing yield. Producing yields of tetrapod whisker was high when the weights of Zn powder was used more than 3.5 g and it seem to be saturated. Producing yield of whiskers did not have a significant change with the change of Zn powder weight used. The obtained whiskers which prepared by thermal oxidation of Zn powder were almost hexagonal column shaped but the higher of weight of
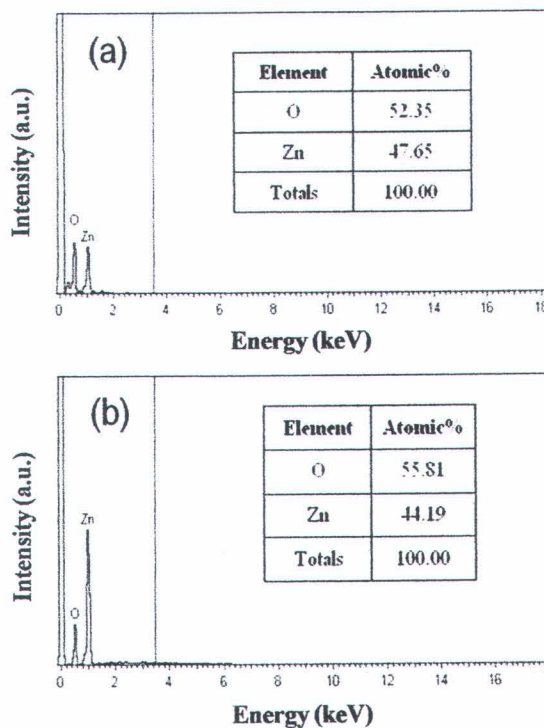
Figure 3. The EDS analysis of (a) whiskers, (b) tetrapod whiskers.
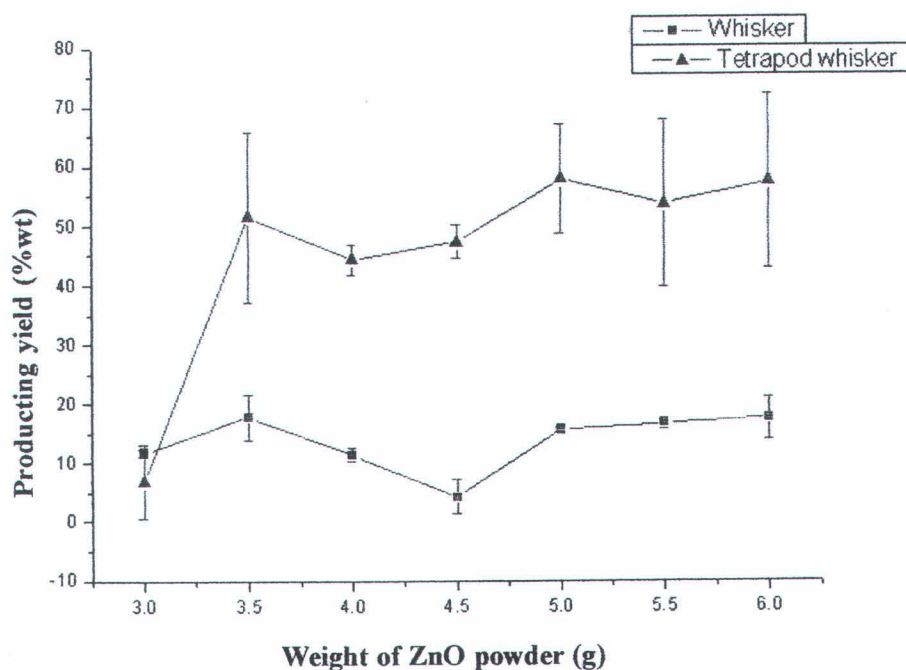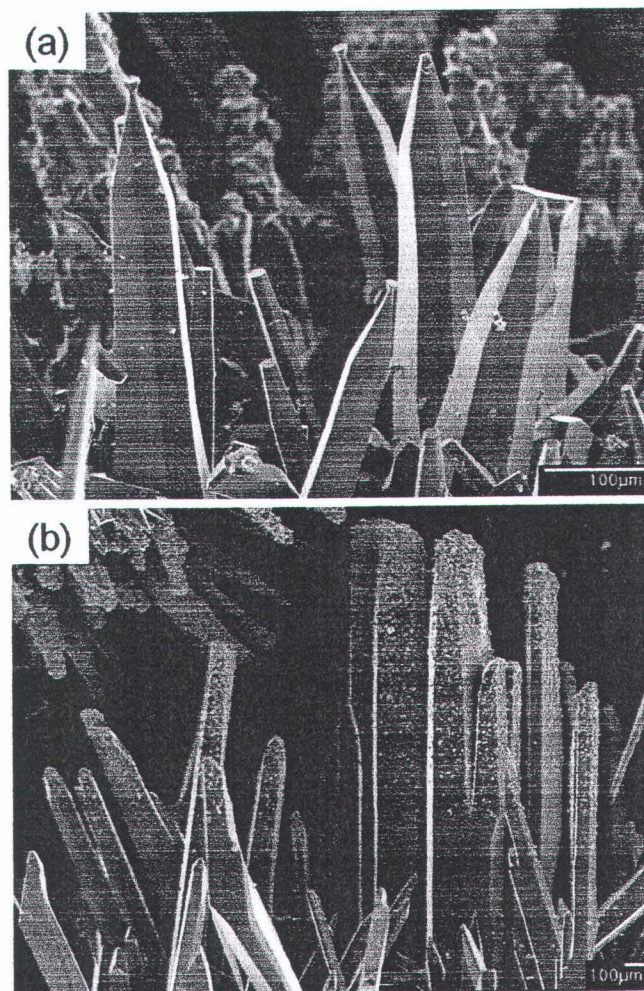

Figure 4. The effect of ZnO powder weight on the producting yield.

Zn powder led to less uniform of structure, as showed in Figure 5. Because of the high vapor pressure of Zn in the growth area, it was found that a lot of fine particles were deposited on the surface of whiskers.

Figure 5. SEM images of ZnO whiskers which different ZnO powder weight used. (a) Zn powder 3.5 g, (b) Zn powder 5 g.

4. CONCLUSIONS

ZnO whiskers were successfully prepared by thermal oxidation method. From FE-SEM, the lengths of whiskers were in the range of 10-240 µm, the diameters were in the range of 0.20 - 4.60 µm while the percent of yield was up to 20% by weight. The lengths of tetrapod whiskers were in the range of 3.15-10.63 µm, the diameters were in the range of 0.13- 2.64 µm while the percent of yield was up to 68% by weight. From EDS, it was suggested that the chemical component is ZnO. It was found that the higher of weight Zn powder led to less uniform of structure.

REFERENCES

[1] Xu J., Chen Y. and Shen J., Solvothermal Preparation and Gas Sensing Properties of ZnO Whiskers, *J. Nanosci. Nanotechnol.*, 2006; **6**: 248-253.

[2] Lyapina O.A., Baranov A.N., Panin G.N., Knotko A.V. and Kononenko O.V., Synthesis of ZnO Nanotetrapods, *Inorg. Mater,* 2008; **8**: 958-965.

[3] Ling J., Chun C., Zhang J., Huang Y., Shi F.J., Ding X.X., Tang Chi. and Qi S.R., Controllable Growth of Zinc Oxide Micro- and Nanocrystals by Oxidation of Zn-Cu Alloy, *J. Solid State Chem.*, 2005; **178**: 819-824.

[4] Xu J., Han J., Zhang Y., Sun Yu' and Xie B., Studies on Alcohol Sensing Mechanism of ZnO Based Gas Sensors, *Sens. Actuators, B,* 2008; **132**: 334-339.

[5] Hwang C.C., Lin C.S., Wang G.P., Peng C.H. and Chung S.L., A Self propagating High temperature Synthesis Method for Synthesis of Zinc Oxide Powder, *J. Alloys Compd.*, 2009; **467**: 514-523.

[6] Iwanaga H., Fujii, M. and Takeuchi S., Growth Model of Tetrapod Zinc Oxide Particles, *J. Cryst. Growth.*, 1993; **134**: 275-280.

[7] Hu J.Q. and Bando Y., Growth and Optical Properties of Single-crystal Tubular ZnO Whiskers, *Appl. Phys. Lett.*, 2003; **82**: 1401-1403.

[8] Cheng J., Guo R. and Wang Q.M., Zinc Oxide Single-crystal Microtubes, *Appl. Phys. Lett.*, 2004; **85**: 5140-5142.

[9] Tsukazaki A., Ohtomo A., Onuma T., Ohtani M., Makino T., Sumiya M., Ohtani K., Chichibu S.F., Fuke S., Segawa Y., Ohno H., Koinuma H. and Kawasaki M., Quantum Hall Effect in Polar Oxide Heterostructures. *Nat. Mater.*, 2005; **4**: 42-48.

[10] Pan Z.W., Dai Z.R. and Wang Z.L., Nanobelts of Semiconducting Oxides, *Science.*, 2001; **291**: 1947-1949.

[11] Li Y., Meng G.W., Zhang L.D. and Phillipp F., Ordered Semiconductor ZnO Nanowire Arrays and Their Photoluminescence Properties, *Appl. Phys. Lett.*, 2000; **76**: 2011–2013.

[12] Sun X.H., Lam S., Sham T.K., Heigl F. and Ju1rgensen A., Synthesis and Synchrotron Light Induced Luminescence of ZnO Nanostructures: Nanowires, Nanoneedles, Nanoflowers and Tubular Whiskers, *J. Phys. Chem. B.*, 2005; **109**: 3120-3125.

[13] Wu J.J., Liu S.C., Wu C.T., Chen K.H. and Chen L.C., Heterostructures of ZnO–Zn Coaxial Nanocables and ZnO Nanotubes, *Appl. Phys. Lett.*, 2002; **81**: 1312-13124.

[14] Huang M.H., Wu Y.Y., Feick H., Tran N., Webber E. and Yang P.D., Catalytic Growth of Zinc Oxide Nanowires by Vapor Transport, *Adv. Mater.*, 2001; **13**: 113-116.

[15] Egashira M., Kanehara N., Shimizu Y. and Iwanaga H., Gas-sensing Characteristics of Li+- Doped and Undoped ZnO Whiskers, *Sens. Actuators, B,* 1989; **18**: 349-360.

[16] Chaiworn P., *Preparation of Zinc Oxide Whisker by Growth from Vapor Method for Ethanol Sensor,* M.S. Thesis, Chiang Mai University, Thailand, 2007.

[17] Greenham N.C., Peng X. and Alivisatos A.P., Charge Separation and Transport in Conjugated-Polymer/Semiconductor-

Nanocrystal Composites Studied by Photoluminescence Quenching and Photoconductivity, *Phys. Rev. B: Condens. Matter Mater. Phys.*, 1996; **54**; 17628–17637.

[18] Jo S.H., Banerjee D. and Ren Z. F., Field Emission of Zinc Oxide Nanowires Grown on Carbon Cloth, *Appl. Phys. Lett.*, 2004; **85**: 1407-1409.

[19] Heo Y.W., Tien L.C., Kwon Y., Norton D.P., Pearton S.J., Kang B.S. and Ren F., Depletion-mode ZnO nanowire field-effect transistor, *Appl. Phys. Lett.*, 2004; **85**: 2274-2276.

[20] Newton M.C. and Warburton P. A., ZnO tetrapod nanocrystals, *Mater. Today,* 2007; **10(5)**: 50-54.

[21] Zhou Z., Deng H., Yi D. and Liu S., A New Method for Preparation of Zinc Oxide Whiskers, *Mater. Res. Bull.,* 1999; **34**: 1563-1567.

[22] Zhou Z., Peng W., Ke S. and Deng H., Tetrapod-shaped ZnO Whisker and Its Composites, *J. Mater. Process. Technol,* 1999; **89-90**: 415-418.

[23] Wang Y.G., Yuen Clement, Lau S.P., Yu S.F. and Tay B.K., Ultraviolet Lasing of ZnO Whiskers Prepared by Catalyst-free Thermal Evaporation, *Chem. Phys. Lett.,* 2003; **377**: 329-332.

[24] Yuan H.T. and Zhang Y., Preparation of Well-aligned ZnO Whiskers on Glass Substrate by Atmospheric MOCVD, *J. Cryst. Growth,* 2004; **263**: 119–124.

[25] Chang Y.S. and Ting J.M., Growth of ZnO Thin Films and Whiskers, *Thin Solid Films,* 2001; **398-399**: 29-34.

[26] Dai Z.R., Pan Z.W. and Wang Z.L., Novel Nanostructures of Functional Oxides Synthesized by Thermal Evaporation, *Adv. Funct. Mater.,* 2003; **13**: 9-24.

[27] Choopun S., Hongsith N., Wongrat E., Kamwanna T., Singkarat S., Mangkorntong P. and Mangkorntong N., Growth Kinetic and Characterization of RF-Sputtered ZnO:Al Nanostructures, *J. Am. Ceram. Soc.,* 2008; **91**: 174 -177.

[28] Hongsith N., Chairuangsri T., Phaechamud T. and Choopun S., Growth Kinetic and Characterization of Tetrapod ZnO Nanostructures, *Solid state Communications.,* 2009; **149**: 1184-1187.

ประวัติผู้เขียน

ชื่อ-สกุล	นายเกียรติภูมิ กองจาย
วัน เดือน ปีเกิด	20 มกราคม 2527
ประวัติการศึกษา	- สำเร็จการศึกษาประดับประถมศึกษาจากโรงเรียนบ้านแม่สูนน้อย ต.แม่สูน อ.ฝาง จ.เชียงใหม่ ปีการศึกษา 2538
	- สำเร็จการศึกษาประดับมัธยมศึกษาตอนต้นจากโรงเรียนรังษีวิทยา ต.เวียง อ.ฝาง จ.เชียงใหม่ ปีการศึกษา 2541
	- สำเร็จการศึกษาประดับมัธยมศึกษาตอนปลายจากโรงเรียนรังษีวิทยา ต.เวียง อ.ฝาง จ.เชียงใหม่ ปีการศึกษา 2544
	- สำเร็จการศึกษาปริญญาตรี สาขาฟิสิกส์ คณะวิทยาศาสตร์ มหาวิทยาลัยเชียงใหม่ ปีการศึกษา 2548
	- สำเร็จการศึกษาประกาศนีบัตรวิชาชีพครู คณะศึกษาศาสตร์ มหาวิทยาลัยเชียงใหม่ ปีการศึกษา 2549